Eur Radiol (2007) 17: 743–761
DOI 10.1007/s00330-006-0404-1

Heike E. Daldrup-Link
Tobias Henning
Thomas M. Link

MR imaging of therapy-induced changes of bone marrow

Received: 2 February 2006
Revised: 30 May 2006
Accepted: 23 June 2006
Published online: 21 September 2006

H. E. Daldrup-Link (✉) · T. Henning · T. M. Link
Department of Radiology,
University of California San Francisco,
505 Parnassus Ave.,
San Francisco, CA 94143-0628, USA
e-mail: daldrup@radiology.ucsf.edu
Tel.: +1-415-4764328
Fax: +1-415-4760616

Abstract MR imaging of bone marrow infiltration by hematologic malignancies provides non-invasive assays of bone marrow cellularity and vascularity to supplement the information provided by bone marrow biopsies. This article will review the MR imaging findings of bone marrow infiltration by hematologic malignancies with special focus on treatment effects. MR imaging findings of the bone marrow after radiation therapy and chemotherapy will be described. In addition, changes in bone marrow microcirculation and metabolism after anti-angiogenesis treatment will be reviewed. Finally, new specific imaging techniques for the depiction of regulatory events that control blood vessel growth and cell proliferation will be discussed. Future developments are directed to yield comprehensive information about bone marrow structure, function and microenvironment.

Keywords Bone marrow · Treatment effects · MR imaging · Contrast agents

Introduction

Bone marrow is the fourth largest organ of the human body. Its main function is the hematopoiesis, i.e., it provides the body with erythrocytes, leukocytes and platelets in order to maintain the oxygenation, immune function and autorestoration of the body.

MR imaging provides a non-invasive visualization of the bone marrow and may be used to define its cellular or fat content as well as its vascularity and metabolism. Treatment effects due to irradiation, chemotherapy or other new treatment regimens may change one or several of these components, thereby causing local or generalized changes in bone marrow signal intensity on MR images. This article will provide an overview over such treatment-related bone marrow signal changes on MR imaging. In order to recognize these treatment effects, one has to be familiar with the MR imaging features of the normal and non-treated pathologic marrow. Thus, this article will first provide a brief overview over MR imaging features of the normal and non-treated pathologic marrow as a basis for subsequent descriptions of the bone marrow after conservative or new treatments.

Indications to study treatment effects

In patients with hematopoietic malignancies the diagnosis of neoplastic bone marrow infiltration is crucial to determine prognosis and to identify suitable treatment protocols [1]. This diagnosis is usually obtained by iliac crest biopsy, which is mandatory for staging and histopathologic classification of the disease [2–4]. In non-Hodgkin's lymphoma (NHL) a neoplastic bone marrow infiltration indicates the highest stage (stage four) according to the Ann Arbor Classification. In cases of myeloma, the extent of bone marrow infiltration may be associated with any stage of the Salmon and Durie classification [2].

In both instances, iliac crest biopsy may be false negative when the bone marrow infiltration is focal rather than diffuse [3, 4].

The role of MR imaging for the depiction of bone marrow infiltration by hematologic malignancies is controversial and depends on the type, stage and clinical course of the malignancy. For patients with multiple myeloma, MR has been established in some centers as an integrative technique for staging and treatment monitoring, since it proved to be highly sensitive for the detection of bone marrow infiltrates and provided important additional information to conventional bone surveys. In several studies, MR showed a higher sensitivity than conventional bone surveys and bone scintigraphy for the detection of focal bone marrow lesions [5, 6]. Thirty-three percent of patients with myeloma were "understaged" based on the skeletal survey when compared to MR [7]. And some MR findings have been shown to have direct prognostic relevance: In patients with stage 1 disease according to Salmon and Durie, a pathologic bone marrow MR and normal bone survey was associated with a worse prognosis than a normal MR and normal bone survey [8, 9]. And in patients with stage 3 disease according to Salmon and Durie, a diffuse bone marrow infiltration, as shown on MR images, was associated with a worse prognosis than a multifocal bone marrow infiltration [10, 11].

For patients with Hodgkin's lymphomas and high-grade NHL, FDG-PET has been established as the imaging modality of choice for staging and treatment monitoring and MR imaging should only be considered in selected cases with high risk of bone marrow involvement and equivocal findings on PET or extracompartmental tumor growth. Neither MR nor FDG-PET is meant to replace marrow biopsy, because the histopathologic subtype of lymphoma has to be defined, and because minimally diffuse, microscopic marrow involvement can be false negative with either imaging technique [12]. On the other hand, routinely performed iliac crest biopsies cover only a small portion of the entire bone marrow and also provide potential false-negative findings [3, 4, 12]. Thus, in selected patients with a high risk of bone marrow involvement, MR imaging may contribute clinically significant information. In a study by Hoane et al. in 98 patients with malignant lymphoma, up to one-third of the patients evaluated with routine iliac crest biopsies had occult marrow tumor detectable with MRI [12]. In addition, patients with negative marrow biopsies but pathologic MR were found to have a worse prognosis than patients with negative marrow biopsies and normal MR [13]. Thus, since the diagnosis of bone marrow involvement affects treatment decisions and prognosis, these authors concluded that optimal bone marrow evaluation in such patients should include both biopsy and MR [12]. Another valuable contribution of MR is its capacity to detect soft-tissue paravertebral masses as well as epidural masses and neural foramen invasion, which may accompany vertebral disease. In case of clinical symptoms such as unexplained back pain or new neurological symptoms, MR is the modality of choice to detect paravertebral and epidural masses, which may accompany bone marrow infiltration of the spine.

For patients with leukemia, there is currently no role for routine bone marrow evaluation with MR imaging, neither before nor after therapy. Particular questions in these patients that may be addressed by MR are the search for biopsy sites in patients with suspected new or relapsed disease, but negative bone marrow biopsy as well as the diagnosis of treatment complications, such as treatment induced bone marrow infarcts or avascular necroses, when conventional radiographs are negative or equivocal [14].

In summary, dedicated MR imaging of the bone marrow in patients with hematologic malignancies is currently restricted to applications in patients with multiple myeloma, selected patients with other malignant lymphomas with a high risk of bone marrow infiltration and/or extracompartmental tumor growth as well as patients with potential treatment complications. Additional patients with hematologic malignancies may undergo MR imaging for evaluations of other pathologies, outside the bone marrow. And since the bone marrow is depicted on nearly any MR examination throughout the body, the knowledge of the normal and pathologic marrow of these patients before and after therapy is crucial for the radiologist in order to provide a comprehensive diagnosis. Such "secondary" evaluations of the bone marrow may outperform above mentioned primary indications in this patient population.

Technique

Standard techniques to depict the bone marrow at 1 T and 1.5 T clinical scanners comprise plain T1-weighted spinecho (SE) or fast-SE (FSE) sequences as well as short TI inversion recovery (STIR) sequences. The T1-weighted, non-fat-saturated spinecho (SE) or FSE sequences are best suited to define the cellular content of the bone marrow and should be included in any protocol for MR imaging of the bone marrow. STIR sequences are useful as a screening sequence to search for abnormalities in the bone marrow, most of which appear with a very high signal intensity on these sequences. There is some debate about the optimal inversion time (TI) for depiction of the bone marrow abnormalities with STIR sequences [15–18]: Some authors prefer a TI that causes a suppression of all normal structures and provides a maximal contrast between normal (no signal) and pathologic (high signal) tissues. Other authors prefer a TI, which is slightly higher in order to provide some additional background signal of normal tissues (low signal), and, thus, improved anatomical information. The advantages of STIR sequences are that they provide a very high tissue contrast and that they are insensitive to magnetic field inhomogeneities. The

disadvantages are that STIR sequences have a limited signal-to-noise ratio and that the fat suppression technique is non-specific: The signal from tissue or fluid with a T1 similar to that of fat will also be suppressed, for example, mucoid tissue, hemorrhage, proteinaceous fluid, and gadolinium [18].

Selective fat-suppressed T2-weighted images are an alternative to STIR-images at high field MR scanners. Selective fat saturation is lipid specific, usually provides a higher signal-to-noise ratio than STIR sequences and does not suppress gadolinium-based contrast agent (i.e., can be added after contrast medium administration). However, selective fat saturation is susceptible to magnetic field inhomogeneities. To achieve reliable fat saturation, the frequency of the frequency-selective saturation pulse must equal the resonance frequency of lipid. Inhomogeneities of the static magnetic field will shift the resonance frequencies of both water and lipid, this discrepancy would result in poor fat suppression or - even worse - saturation of the water signal instead of the lipid signal. Static field inhomogeneities inherent in magnet design are relatively small in modern magnets and can be reduced by decreasing the field of view, centering over the region of interest, and autoshimming. However, substantial inhomogeneities can be caused by local magnetic susceptibility differences such as those found at air-bone interfaces or around foreign bodies like metal or air collections [18]. Of note, T2-weighted FSE sequences without fat saturation are probably the worst sequences for evaluation of the bone marrow since both lesions and normal fatty marrow appear hyperintense on these sequences.

Other MR imaging techniques have been developed to improve the detection and quantification of diffuse bone marrow involvement. These techniques include chemical-shift imaging, bulk T1 relaxation time measurement, and hydrogen 1 spectroscopy [19]. All of these methods were used to measure the fat content or the water/fat fraction more accurately. However, these measurements have so far not demonstrated clinical significance, and hence these techniques are currently not used for routine imaging.

Diffusion-weighted MR imaging techniques have been reported to be useful for the differentiation of neoplastic marrow infiltration and pathologic vertebral fractures [20]. Recently, further advanced diffusion-weighted whole body scans have been described for treatment monitoring of patients with leukemia [21]. The technique relies on selective excitation of the water resonance and generation of image contrast that is dependent upon differential nuclear relaxation times and self-diffusion coefficients.

Contrast-agent enhanced scans In most instances, the administration of Gd-based contrast agents is not necessary for evaluation of bone marrow disorders. Administration of Gd-DTPA can be helpful to differentiate cysts and tumors, to differentiate necrotic and viable tumor tissue before a biopsy, in suspected osteomyelitis or in equivocal cases of bone infarcts. If Gd-DTPA-enhanced scans are performed, fat saturated T1-weighted sequences should be used in order to suppress the fatty components of the bone marrow with intrinsic high signal intensity and, thus, to provide an optimal depiction of the Gd-enhancement.

The diagnosis of lesion vascularization based on comparisons between plain **non**-fat-saturated and fat-saturated, Gd-enhanced T1-weighted sequences is no problem, if the investigated focal lesion shows a marked enhancement. However, it may be difficult to determine, if a certain lesion shows minimal or no contrast enhancement based on comparisons of plain **non**-fat-saturated and fat-saturated Gd-enhanced sequences. In these cases, we recommend to obtain additional Gd-enhanced **non**-fat-saturated T1-weighted MR sequences with identical pulse sequence parameters as the plain sequences. A subtraction of pre and post sequences can then identify a presence or absence of contrast enhancement of certain focal lesions, listed above.

Additional dynamic, contrast enhanced scans after administration of Gd-DTPA have been applied by some investigators in order to generate estimates of the blood volume of the normal or pathologic bone marrow before and after treatment [22, 23]. Such dynamic contrast enhanced MR studies with gadolinium chelates should be performed with rapid acquisition techniques, producing interscan intervals as short as possible, to best measure the rapidly evolving distribution patterns of these small molecular probes (<600 daltons). Although investigated since 1993 [23], dynamic Gd-DTPA-enhanced MR studies have not shown clinical significance so far. In addition to bone marrow perfusion, the amount of contrast agent at any time within the bone marrow depends on several additional inter-related variables including microvessel permeability, endothelial surface area, hydrostatic pressure, osmotic pressure, diffusion, convective forces, interstitial pressure and clearance. Clearly, contrast media kinetics in the bone marrow is not a simple matter and shows a high interindividual and intraindividual variability with respect to the mentioned influencing factors [24–26]. This may be one reason why it did not find wide clinical application to date.

New, macromolecular contrast media (MMCM) may provide more specific information on bone marrow blood volume and sinus permeability, which may be more useful to study treatment effects. Small molecular Gd-chelates can only estimate the blood volume (immediate post-contrast scans) and extracellular space (later post-contrast scans) of the normal or abnormal bone marrow, because these small molecules permeate readily and non-selectively across normal and abnormal capillaries in the bone marrow. MMCM can also estimate the blood volume based on immediate post-contrast scans. In addition, MMCM are so large that their diffusion across microvessels is affected by the permeability of these vessels. This may be helpful for

treatment monitoring of anti-angiogenesis drugs, which specifically and readily decrease microvascular permeability, but which have no immediate effect on the blood volume. Thus, MMCM may be able to predict a response to anti-angiogenic treatment before a subsequent arrest in tumor vessel growth (decrease in blood volume) and before clinical signs of response (laboratory parameters) are apparent [27]. At this time, none of the MMCMs are yet FDA approved, but several of these agents are currently in advanced stages of development for applications in patients (phase II and III clinical trials), such as MS-325/Vasovist (Epix and Schering, approved in Europe), Gadomer-17 (Schering), SHU555C (Schering), Sinerem/Combidex (Guerbet/Advanced Magnetics), B-22956/1 (Bracco) and Code 7228 (Advanced Magnetics). In order to acquire useful kinetic information from MMCM-enhanced studies, a series of images spanning at least 20–30 minutes after contrast medium administration, is required [27]. On the other hand, since the transendothelial diffusion of MMCM is a rather slow process, it is usually sufficient to acquire MMCM-enhanced dynamic data with intervals of one to two minutes or, for specific questions, even to obtain just one delayed contrast enhanced scan. Applications of potential clinical interest will be mentioned in the specific sections below.

One new class of contrast agents, particularly noteworthy with respect to bone marrow imaging, is the group of ultra small superparamagnetic iron oxide particles (USPIO). These particulate iron oxide contrast agents are phagocytosed by macrophages in the normal bone marrow, where they induce a T2-shortening effect. The principle is similar to MR imaging of the liver with superparamagnetic iron oxide particles (SPIO). However, SPIO, used for liver imaging have a diameter of >50 nm, whereas USPIO used for bone marrow imaging have a diameter of <50 nm. USPIO particles are not taken up in neoplastic marrow infiltrates, which do not contain macrophages [28–30]. Thus, USPIO may be used to differentiate hypercellular normal and neoplastic marrow. After infusion of USPIO at a dose of 2.6 mg/kg body weight, the normal marrow shows a USPIO induced signal loss as opposed to focal neoplastic infiltrates, which do not show any signal loss, and, thus, stand out as bright lesions [17, 29, 31]. STIR- or T2-weighted fat saturated sequences are best suited for such USPIO-enhanced MR scans. Metz et al. found a significantly increased number of detected focal bone marrow lesions (<1 cm) in patients with lymphoproliferative disorders on these sequences after administration of USPIO compared to non-enhanced scans [17]. The USPIO Ferumoxtran-10 (Sinerem/Combidex, Guerbet / Advanced Magnetics) is expected to become approved for clinical applications in 2006 in Europe and has already shown its ability to differentiate normal and pathologic hypercellular marrow and to detect multifocal lesions within the bone marrow [17, 31]. Other USPIOs, which are in different stages of preclinical and clinical trials are SHU555C/ Resovist S (Schering), Code 7228 (Advanced Magnetics), VSOP (Ferropharm) and Clariscan (Amersham/GE).

Future imaging developments are likely to generate combined techniques that will maximize the information to be extracted from the image. Tumor location, morphology and function will be integrated. For example, both dynamic contrast-enhanced MR imaging and MR spectroscopy can be acquired in a single diagnostic session to define bone marrow vascular and metabolic characteristics [32].

New developments for whole body MR imaging, such as parallel imaging techniques, dedicated coils (Angio-SURF), and the total imaging matrix (Siemens systems, Avanto) may provide a “screening” of the whole red bone marrow for tumor infiltration within a reasonable time.

Additional development is being directed towards combined PET and MR imaging, either by retrospective spatial registration of data from PET and MR images, obtained on separate PET and MR machines or by sequential data acquisitions on combined PET-MR scanners [33, 34]. PET-MR imaging has been described as superior, a least for some applications, compared to PET-CT because of the improved intrinsic soft tissue contrast and potential direct bone marrow depiction provided by MR.

Normal bone marrow

The normal bone marrow undergoes age-related changes of its cellular content with increasing age of the patient. In adults, the normal bone marrow is characterized by a partial or complete fatty conversion and low cellularity, which leads to a relatively high signal intensity on plain T1-weighted images and low signal intensity on STIR- or fat saturated T2-weighted MR images [35–38]. In children, the normal bone marrow is highly cellular, which leads to a low signal intensity on plain T1-weighted images and high signal intensity on STIR- or fat saturated T2-weighted MR images. With increasing age, a conversion from this highly cellular marrow in children to fatty marrow in adults occurs with a gradual increase of the bone marrow signal on T1-weighted MR images and a gradual decline of the bone marrow signal on STIR- or fat saturated T2-weighted MR images over time. This conversion also follows a particular distribution pattern within the skeleton: it starts in the peripheral skeleton and progresses centrally [38]. Within long bones, it first involves the epiphyses, then the diaphyses and, finally, the metaphyses [38]. In the vertebrae, it starts in the center, around the venous plexus, and progresses peripherally [38]. In adults, the signal intensity of the normal bone marrow is typically hyperintense to surrounding muscle and intervertebral disks on T1-weighted MR images and hypointense to surrounding muscle on STIR- or fat saturated T2-weighted MR images. The knowledge of this pattern of conversion is useful to differentiate normal cellular marrow from focal or diffuse

neoplastic involvement and to recognize treatment effects and tumor recurrence.

The enhancement of the normal bone marrow in healthy persons after administration of standard small molecular Gd-chelates can vary greatly (range 3-59%, mean 21%, SD 11%) and decreases with increasing age [26]. As a rule of thumb, a signal Gd-enhancement of less than 40% on T1-weighted MR images was reported to be normal in adults of more than 40 years. However, this threshold is dependent on the applied field strength and pulse sequence parameters. The relative enhancement of both normal and abnormal marrow may be higher with new, more sensitive pulse sequences [25]. Thus, each investigator should establish the specific threshold for normal bone marrow enhancement for the technique used at his particular MR scanner and institution.

Pathologic bone marrow in hematologic malignancies

Neoplastic infiltration of the bone marrow in MR images results in a replacement of the fatty converted marrow by neoplastic cells, thereby increasing the cellular content of the bone marrow, which results in a prolongation of T1- and T2-relaxation times and subsequent decreased T1-signal and increased T2-signal of the bone marrow. The detection of neoplastic bone marrow infiltrations with MR imaging depends on the quantity and distribution of cellular infiltration.

The distribution of neoplastic bone marrow involvement in patients with hematologic malignancies may be focal, multifocal or diffuse. In patients with NHL, a focal or multifocal involvement is more common than the diffuse infiltration pattern. In patients with myeloma, an additional, typical “salt and pepper” or variegated distribution may be observed, most frequently in stage I disease according to Salmon and Durie. In patients with leukemia, the bone marrow is usually involved in a diffuse fashion. A multifocal involvement may be seen in a small proportion of patients, particularly those with AML.

The detection of focal, multifocal and “salt and pepper” or variegated infiltrations of the bone marrow in patients with NHL is straight forward: The MR signal intensity of focal bone marrow lesions is typically iso- or hypointense to surrounding muscle and intervertebral disks on T1-weighted MR images and hyperintense to surrounding muscle on STIR- or fat saturated T2-weighted MR images. Since these focal lesions are also associated with an increased angiogenesis, they show an increased signal enhancement compared to the surrounding bone marrow on fat saturated T1-weighted MR images.

The detection of a diffuse bone marrow infiltration with MR imaging is limited. Using standard MR scanners and pulse sequences, an infiltration of the bone marrow with more than 30% of neoplastic cells can be readily detected by a diffusely decreased T1-signal and a diffusely increased T2-signal [39]. An infiltration with less than 20% neoplastic cells cannot be distinguished from normal marrow with standard MR pulse sequences. Several authors reported a normal bone marrow MR signal in patients with leukemia, in patients with early stages of bone marrow invasion by lymphoproliferative diseases and even in up to one-quarter of patients with stage III multiple myeloma [40].

The administration of Gd-DTPA is not necessary for staging of focal, multifocal and “salt and pepper” lesions, which can be readily detected on plain MR scans. Dynamic Gd-DTPA-enhanced MR scans documented repetitively an increased blood volume (i.e., increased enhancement) of neoplastic infiltrations compared to the normal bone marrow [22, 23, 41]. As one would expect, the Gd-enhancement was significantly higher in marked bone marrow infiltrations than in mild or no infiltration ($P<0.05$) and the enhancement was higher in lesions with high vessel-density than in lesions with low vessel-density at histology ($P=0.01$). In addition, a higher enhancement was found in the presence of increased serum immunoglobulins [42]. However, the Gd-DTPA enhancement of focal neoplastic lesions has not shown additional clinically significant information for staging purposes so far. In some cases, Gd-administration may help to diagnose a diffuse bone marrow infiltration. According to studies from Staebler et al., a bone marrow signal intensity increase exceeding 40% indicates a diffuse infiltration in adult patients [43].

Irradiation

MR signal changes of the bone marrow during and after irradiation are time and dose dependent: In the acute phase (day 1–3 of irradiation), the bone marrow develops an edema, which appears hypointense on T1-weighted MR images and hyperintense on fat-saturated T2-weighted and STIR-images. Contrast enhanced T1-weighted images show a transiently increased enhancement of the bone marrow during this phase. Subsequently (day 4–10), focal T1-hyperintense and T2/STIR-hypointense areas of hemorrhage may occur. The bone marrow ultimately undergoes a conversion to fatty marrow, which closely represents the irradiation field and which appears very bright on T1-weighted MR images (close to subcutaneous fat) and dark on fat suppressed images (Fig. 1). Dependent on the applied dose, this fatty transformation of the bone marrow may be detected with MR imaging as early as 10–14 days after therapeutic irradiation [44]. In other cases, the edema may persist for weeks and a fatty conversion may only become apparent months after the irradiation. This fatty conversion is reversible after an irradiation of less than 30–40 Gy and irreversible after an irradiation with more than 40 Gy. The time frame of reconversion after low dose irradiation has not been specified so far and will be most

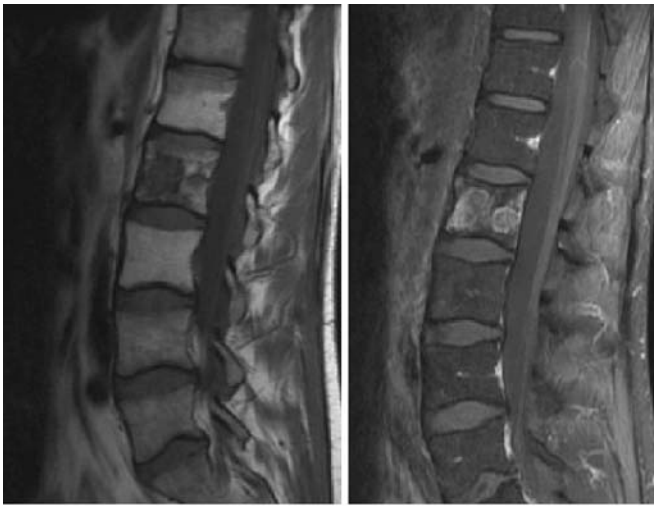

Fig. 1 T1-weighted non-enhanced (**a**) and fat saturated contrast enhanced (**b**) MR images after radiation therapy of a focal PNET tumor infiltration in L 2. Note the fatty conversion of the bone marrow in the irradiation field, L1 to L3, is only apparent on the non-fat saturated non-enhanced MR image. The tumor in L2 shows a mild Gd-enhancement after radiotherapy on contrast-enhanced scans

likely highly variable with respect to potential additional chemotherapy or GCSF-treatment, location and extend of the affected anatomical area and age of the patient. Contrast enhanced scans show a markedly decreased enhancement of the fatty converted bone marrow.

In addition to these bone marrow signal changes in the irradiation field, several authors also reported an additional small, but measurable fatty conversion of the adjacent bone marrow, outside of the irradiation field. The bone marrow outside the irradiation field showed similar MR signal intensity changes compared to the bone marrow within the irradiation field, but to a much lower degree. Interpretations of these findings differ, the most appealing explanation is a fatty conversion due to scatter irradiation [45, 46].

In children, irradiation may also cause impairment or stop in skeletal maturation. Local irradiation may impair the growth at the growth plate of the irradiated bone after doses as little as 1.3 Gy [47]. In parallel to the above described changes of the bone marrow in general, the metaphyses and growth plates of the affected bones may also show an edema on MR images initially, and, later, a fatty conversion. The severity of impairment in bone growth is dependent on the age of the patient at the time of the irradiation and the administered dose. High doses may lead to marked epimetaphyseal deformities. The affected metaphyses of long bones may show horizontal or longitudinal areas of signal loss of on T1- and T2-weighted MR images, which resemble metaphyseal bands and striations seen on conventional radiographs [47]. Irradiation of the spine may cause a scoliosis, which is typically concave to the irradiation field, if only one side of the spine was irradiated. In children, irradiation of the whole spine may also result in a scoliosis. There is usually an associated impairment of the growth of paraspinal muscles as well as an impaired vertical growth of the irradiated vertebrae. Depending on the applied dose, the bone marrow of the vertebrae may undergo a usually transient or (rarely) persistent fatty conversion and the bone marrow in the peripheral skeleton may show a compensatory hypercellularity.

Irradiation of the brain in children with acute leukemia may result in growth arrest due to a deficiency in growth hormone [47]. In these patients, the bone marrow usually appears normal (in case of remission of the leukemia) on MR images.

In children, irradiation of the proximal femur may cause a slipped capital epiphysis [47]. This may be diagnosed early on MR images by an asymmetry and typical widening of the center or posteromedial region of the affected physis, which is best seen on plain T1-weighted MR images. A potential subsequent closure of the physis may be diagnosed by sequential MRI, it typically develops from the posterior portion anteriorly.

In adults, a short-term complication of local irradiation may be the development of an “irradiation osteitis”, which presents as a T1-hypointense, T2/STIR-hyperintense, inhomogeneous edema on MR images in the irradiation field and which shows a narrow zone of transition to the adjacent, non-irradiated bone marrow. There is no associated extraosseous soft tissue mass. The irradiation osteitis may be associated with insufficiency fractures, which may sometimes be better apparent on MR and sometimes be better apparent on conventional radiographs. Thus, imaging of a suspected irradiation osteitis should always also include conventional radiographs of the affected bone. Irradiation osteitis is rare in children [47].

Other short-term complications of irradiation are insufficiency fractures and avascular necroses (AVN) in the irradiated bone. Insufficiency fractures are caused by normal stress on weight-bearing bones with an irradiation-induced decreased elastic resistance. Depending on the acuteness of the fracture and the time interval after irradiation, MR may show a more predominant edema or a more predominant fatty conversion of the bone marrow. The fracture line may be seen as a bright line on T2-weighted and contrast enhanced T1-weighted MR images, if it is surrounded by adjacent marrow edema (Fig. 2). AVN is caused by an irradiation induced arteritis with fibrosis and endothelial proliferation, blocked arterial inflow or venous outflow, rise in intramedullary pressure, compromised perfusion, and, finally, anoxia and death of bone marrow cells. The MR imaging findings of AVN are described in detail below.

As long-term complications, benign or malignant tumors may occur after irradiation of the bone and bone marrow. Osteochondromas are the most common tumors that may

Fig. 2 Coronal fat saturated T2-weighted (3200/50 ms) (**a**), T1-weighted (600/20 ms) (**b**) and fat saturated T1-weighted (600/20 ms) contrast-enhanced (**c**) MR images of the knee of a 16 year-old patient who underwent radiation therapy of the lower femur and poplitea region. Note fatty bone marrow conversion and fracture lines at the distal femur and proximal tibia (arrows) consistent with irradiation induced insufficiency fractures

develop after total body irradiation (TBI). The irradiation induced development of osteochondromas is inversely related to the age of the patient at the time of the TBI. In children, osteochondromas developed in about 6–18% after TBI. The latency for the development of osteochondromas after TBI is highly variable, but generally shorter than the latency for the development of malignant tumors [48]. On MR imaging, a continuity of the bone marrow space with the lesion and a cartilage cap with a thickness of not more than 3 mm are criteria to prove a benign osteochondroma and to exclude a malignancy. Of note, sarcomatous degeneration of an irradiation induced osteochondroma is extremely rare, although incidental cases have been reported [49]. Other benign bone tumors that may develop after TBI are fibrous dysplasia and aneurysmal bone cysts [48].

Radiation-induced sarcoma is a rare late complication of irradiation, which develops after a latency period of about 10 years in the previous irradiation field. Irradiation induced sarcomas are not directly related to the local radiation dose. Osteosarcomas, fibrosarcomas, malignant fibrous histiocytomas, and other sarcomas may occur [50, 51].

Cortisone treatment

Ischemic (avascular) necrosis is a well recognized complication of high dose cortisone treatment, seen in 1–10% of patients in the initial treatment phase for leukemias or lymphomas (Fig. 3). In addition, AVN occurs in 10% of long-term survivors of bone marrow transplantation (Fig. 4) who received high doses of steroids for the prevention or treatment of graft-versus-host disease. AVN has been also described after chemotherapy or irradiation [47]. The apparently increasing prevalence of this complication may be due to increasing recognition based on increasing use of MR imaging.

AVN is caused by vascular insufficiency, compromised bone marrow perfusion, and, finally, anoxia and death of bone marrow cells. Bones with end-arterial vascular supply and poor collaterals are particularly prone to develop an AVN, such as the femoral head, distal femur and proximal tibia, proximal humeri, tali, scaphoid, and lunate bones.

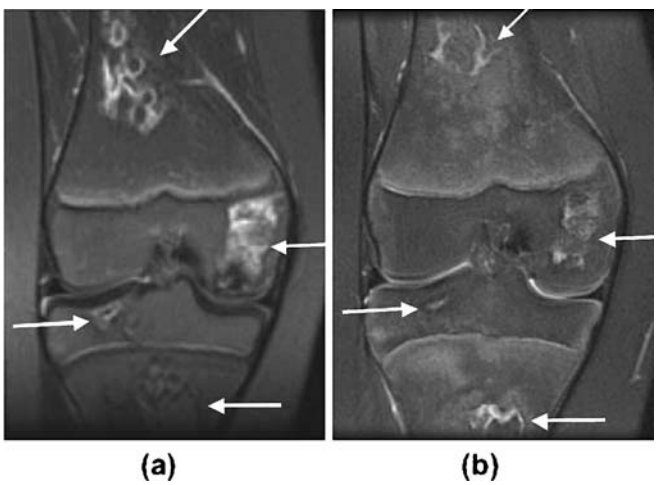

Fig. 3 Coronal fat saturated Spinecho (3200/46 ms) MR images of the knee joint of a 13 year old boy with ALL after treatment with high dose cortisone. There are multiple bone infarctions in the distal femur and proximal tibia (arrows). MR studies were obtained 14months (**a**) and 28 months(**b**) after onset of treatment. Note that the infarcts decrease in size

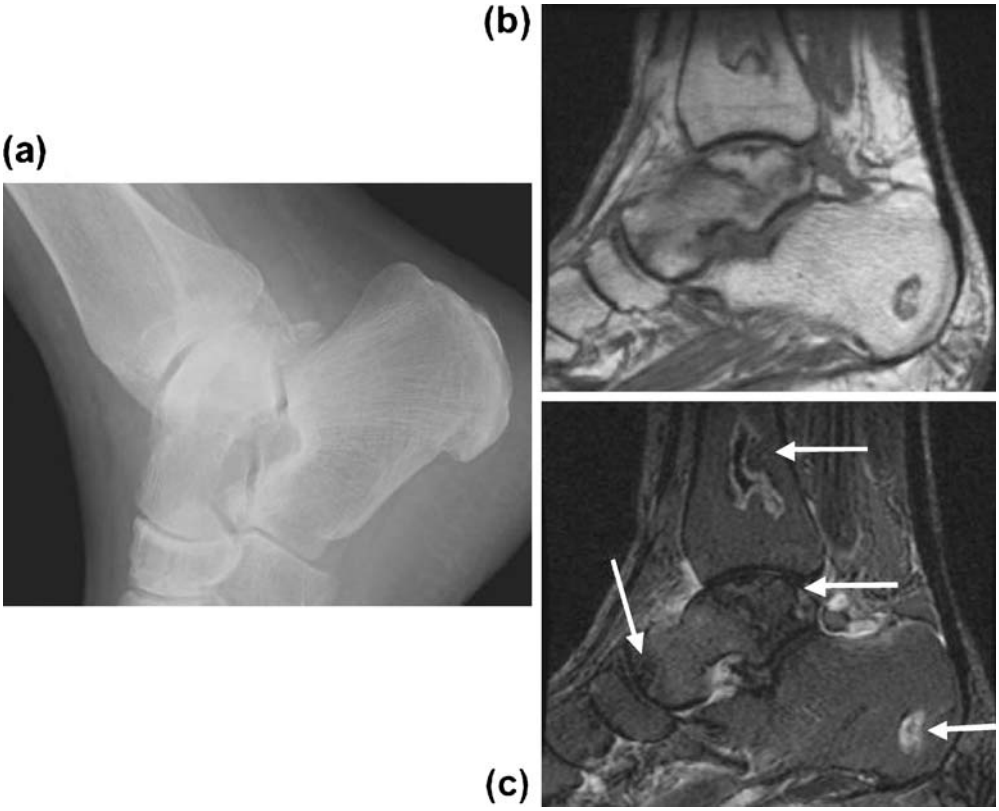

Fig. 4 Conventional radiograph (**a**), sagittal T1-weighted (600/20 ms) (**b**) and sagittal STIR sequence (4000/70 ms, TI: 150 ms) (**c**) of the ankle in a patient with a history of chronic myeloid leukemia and bone marrow transplantation, showing multiple infarcts in the distal tibia, the talus and the calcaneus (arrows), which are not visualized on the radiograph

Usually, the cartilage is not affected because it is nourished by synovial fluid.

MRI is the most sensitive non-invasive method for diagnosis of bone marrow infarction. Early forms of AVN are characterized by a diffuse marrow edema. These T1-hypointense and T2-hyperintense areas of edema may be extensive and are non-specific in their MR appearance. Potential causes, which may all be related to steroid administration, are transient osteoporosis, osteomyelitis, occult intraosseous fracture, and stress fracture. However, in patients under high dose steroid treatment, these areas of edema may represent an early stage of AVN and should be considered a marker for potential progression to advanced osteonecrosis. Therefore, careful examinations for osteonecrosis are necessary when bone marrow edema is seen is these patients [52].

The classic MR appearance of advanced bone marrow infarction is characterized by a segmental area of low signal intensity in the subchondral bone on plain T1-weighted pulse sequences, outlining a central area of marrow, which may have variable signal intensities [53]. This crescentic, ring-like well defined band of low signal intensity on T1-weighted images is thought to represent the reactive interface between the necrotic and reparative zones and typically extends to the subchondral plate. On T2-weighted images, this peripheral band classically appears hypointense with an adjacent hyperintense line - the "double line sign". The hyperintense inner zone represents hyperemic granulation tissue, the hypointense outer zone represents adjacent sclerotic bone. Though characteristic of AVN, this sign is uncommon with the use of fast spin-echo sequences with or without fat suppression and is not necessary for diagnosis of the disease. There is no need to perform conventional T2-weighted sequences to find this sign. On STIR images, the band-like signal alterations of the bone marrow (corresponding to the "inner zone") usually appear hyperintense.

Mitchell et al. described four stages of AVN based on MR imaging findings [54]. The knowledge of these stages may be helpful in the recognition of AVN. Class A lesions had signal intensity characteristics analogous to those of fat, i.e., high signal intensity on T1-weighted images and intermediate signal intensity on T2-weighted images. Class B lesions demonstrated signal intensity characteristics similar to those of blood, i.e., high signal intensity on both T1- and T2-weighted images. Class C lesions had signal intensity properties similar to those of fluid, i.e., low signal intensity on T1-weighted images and high signal intensity on T2-weighted images. Class D lesions had signal intensity properties similar to those of fibrous tissue, i.e., low signal intensity on both T1- and T2-weighted images (2). Class A signal intensity tended to reflect early disease, and class D signal intensity tended to reflect late disease. However, these stages may not occur in a chronological order and did not show prognostic significance [53, 54].

There is currently no established role for Gd-administration in non-traumatic AVN.

Of note, in children, the proximal femur epiphyses may show a residual, small subcortical rim of hematopoietic marrow, which typically appears brighter than adjacent muscles on plain T1-weighted MR images. This should not be confused with the "double line sign" in early AVN, which is characterized by a subcortical rim, which is iso- or hypointense compared to surrounding muscle.

The percentage of the affected weight bearing surface occupied by the AVN is the most reliable factor for predicting outcome [52]. AVN that are entirely circumscribed, and that do not extend cranially to the cortical subchondral margin, have a good outcome, independent of the overall size of the AVN lesion. AVN that do extend to the subchondral margin and are associated with epiphyseal collapse are at risk to result in permanent disability.

AVN may present in an atypical fashion. For example AVN of the spine typically involves a single vertebrae. The MRI findings of a wedge-shaped lesion with fluid intensity (hyperintense signal, like that of cerebrospinal fluid on T2-weighted images) are characteristic for AVN. However, AVN may involve two contiguous vertebrae and the intervening disc and can then be confused with infective or neoplastic processes [55].

Chemotherapy

Chemotherapy in patients with leukemia results in typical signal changes of the bone marrow on MR images, which reflect the underlying changes in the cellular composition and vascularity of the bone marrow [56–58]. During the first week of treatment, the bone marrow sinus becomes dilated and hyperpermeable, leading to an edema. The edematous bone marrow shows a low signal intensity on plain T1-weighted MR images and a high signal intensity on plain T2-weighted and STIR-images. This bone marrow edema was reported to be more pronounced in patients with AML than in patients with ALL, probably reflecting the higher bone marrow toxicity of the chemotherapeutic drugs applied for the treatment of AML (e.g., cytosine arabinoside, which has a known high bone marrow toxicity) as opposed to ALL. Subsequently, a marked decrease in bone marrow cellularity and a fatty conversion of the bone marrow develops, which is characterized by an increase in T1- and T2-relaxation times, an increased signal intensity on plain T1-weighted MR images (Fig. 5) and decreased signal intensity on fat saturated T2-weighted and STIR-images. After successful therapy, a normalization of the MR signal occurs with regeneration of normal hematopoietic cells in the bone marrow. This regeneration often occurs in a multifocal pattern, i.e., within the fatty converted marrow, multiple diffuse small foci of decreased signal on T1-weighted images and increased signal on T2- or STIR-images develop.

Hodgkin's and non-Hodgkin's lymphomas, low- and high-grade lymphomas as well as distinct subgroups of NHL differ markedly in response to treatment. In Hodgkin's lymphoma, a bone marrow infiltration at diagnosis is rare and expected to resolve after treatment. Patients with residual active bone marrow lesions need additional, dedicated treatment. MR is non-specific in differentiating residual viable from non-viable disease. FDG-PET or (in equivocal cases) biopsy are preferable diagnostic methods to answer these questions. There are about 30 subtypes of NHL. About 30% of patients with NHL develop a diffuse large B-cell lymphoma, an aggressive B-cell lymphoma. About 20% of patients with NHL develop a follicular lymphoma, an indolent B-cell lymphoma [59]. About 6% of patients with NHL develop a mantle cell lymphoma, an aggressive B-cell lymphoma that is often widespread at diagnosis. Low-grade lymphomas are considered incurable and are often followed by "watchful waiting". The aggressive high-grade lymphomas are treated with aggressive therapy regimens, chemother-

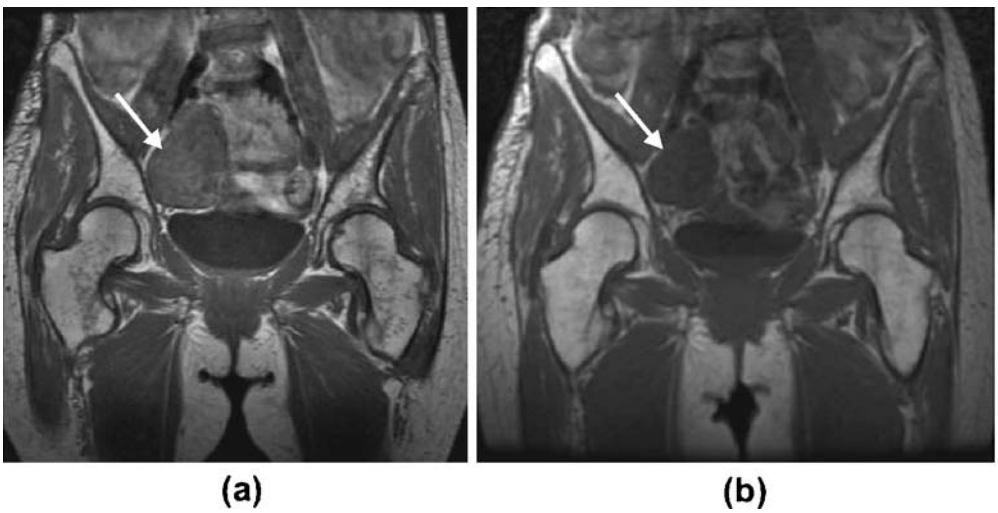

Fig. 5 Coronal T1-weighted spinecho (600/20 ms) images of the pelvis before (**a**) and after (**b**) chemotherapy for a fibrosarcoma of the pelvis (arrow). Note a decrease of hematopoietic bone marrow and an increased fatty conversion in the pelvis and bilateral proximal femurs, while the tumor size shrinks

apy, irradiation, often a combination of both and/or autologous bone marrow transplantation. Bone marrow lesions in these patients are expected to change under therapy on MR images. In general, MR images of patients with Hodgkin's lymphoma and NHL, including myeloma, show a conversion from hypercellular, hypervascularized to normocellular and less vascularized marrow after chemotherapy. However, the "ideal" evolution from hypercellular to normocellular marrow may not occur in all patients with malignant lymphomas. Rahmouni et al. reported that the marrow often returned to normal after treatment when the pattern was diffuse or variegated before treatment [60]. But residual signal alterations of the bone marrow have been also reported after the end of therapy, particularly in patients with a focal pattern before treatment (Fig. 6) [60]. A conversion of a diffuse to a focal MR imaging pattern of marrow involvement, reduction, but not disappearance in lesion size and number, and persistant peripheral lesion enhancement on contrast-enhanced MR images (Fig. 6) have been described in association with a response to standard chemotherapy [58, 60]. In addition, focal bone marrow lesions in patients with lymphoma may show a persistent abnormal signal and/or a cystic or fatty degeneration: A fatty or cystic conversion of focal lesions has been reported as an indication for a response to treatment (Fig. 7) [61]. Low signal intensity on post-therapeutic T2-weighted images is usually associated with fibrosis and rules out relapse. A persistent intermediate hyperintense signal of focal bone marrow lesions on T2-weighted MR images (non-cystic, non-fatty) has been described in association with treatment induced necrosis and inflammation and was found in both responding and non-responding patients [60].

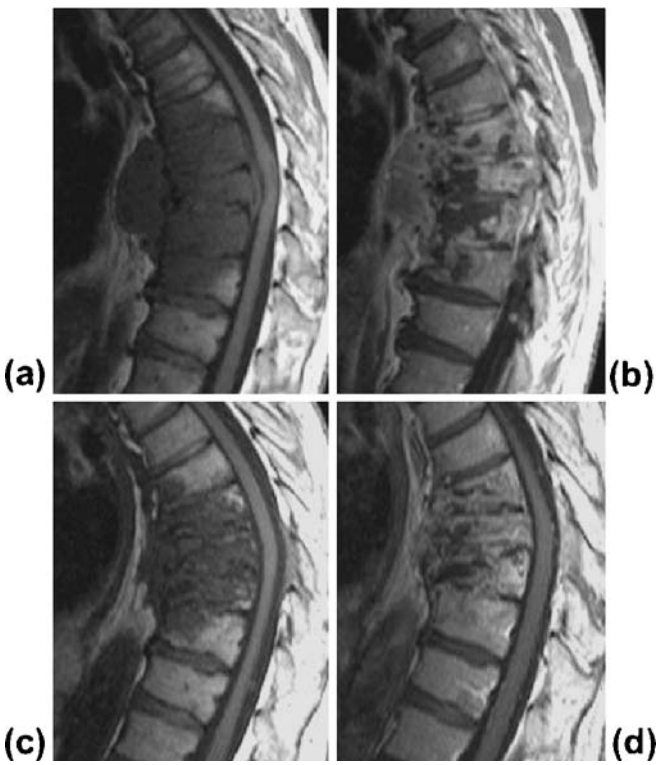

Fig. 6 Sagittal T1-weighted Spinecho sequences (500– 700/15–25 ms) with (**a**, **c**) and without (**b**, **d**) contrast before (**a**, **b**) and after **c**, **d**) chemotherapy for lymphoma. Note decrease in size of the soft tissue component after chemotherapy, yet still significant contrast enhancement in the bone marrow

In patients with myeloma, new or progressive vertebral compression fractures may occur as a complication of treatment response in vertebrae that had extensive marrow disease before treatment [58]. With response to treatment, the tumor mass that had replaced the trabeculae, may resolve and the unsupported vertebrae can collapse. An increasing back pain in patients with myeloma after treatment may be caused by such vertebral compression fractures or tumor progression. Relapse and poor response to treatment are well evaluated with MR imaging. In patients with clinical relapse, new focal lesions, an increase in the size of previously identified focal lesions or a change from focal to diffuse infiltration may be seen. Additional signs of tumor progression are increasing paraosseous soft tissue masses or increased Gd-enhancement of focal lesions after chemotherapy. A progress of focal to diffuse bone marrow neoplasias may be sometimes more difficult to assess, since a diffuse bone marrow infiltration may be indistinguishable from reconverted hematopoietic marrow after e.g., GCSF-treatment. As specified above, a new Gd-enhancement of >40% or lack of USPIO uptake in a hypercellular marrow may indicate a tumor progress or recurrence in these cases.

A rare form of progression in myeloma under therapy is leptomeningeal spread within the central nervous system, reported in 18 out of a series of 1856 patients [62]. MR findings of leptomeningeal enhancement in the brain or spine helped to establish the diagnosis, which was subsequently confirmed by cytologic analysis of cerebrospinal fluid. Myelofibrosis and amyloidosis can also develop as a consequence of treatment in patients with myeloma. Myelofibrosis can be suggested on MR studies as a conversion of the entire bone marrow to diffuse hypointensity on both T1-weighted and STIR images. Amyloidosis can be seen as focal areas of hypointensity on both T1-weighted and STIR images [63].

Perfusion studies using MR enhanced with standard small molecular Gd-based contrast agents provide functional information concerning the response of bone marrow neoplasias to chemotherapy. Conventional cytotoxic drugs have direct or indirect effects on angiogenesis and cause a decrease in bone marrow contrast medium uptake within weeks or months [22, 23, 41]. However, though these techniques are clinically available for more than a decade, perfusion studies are used infrequently or not at all in clinical practice since the obtained functional changes in bone marrow vascularity do not or only slightly precede the

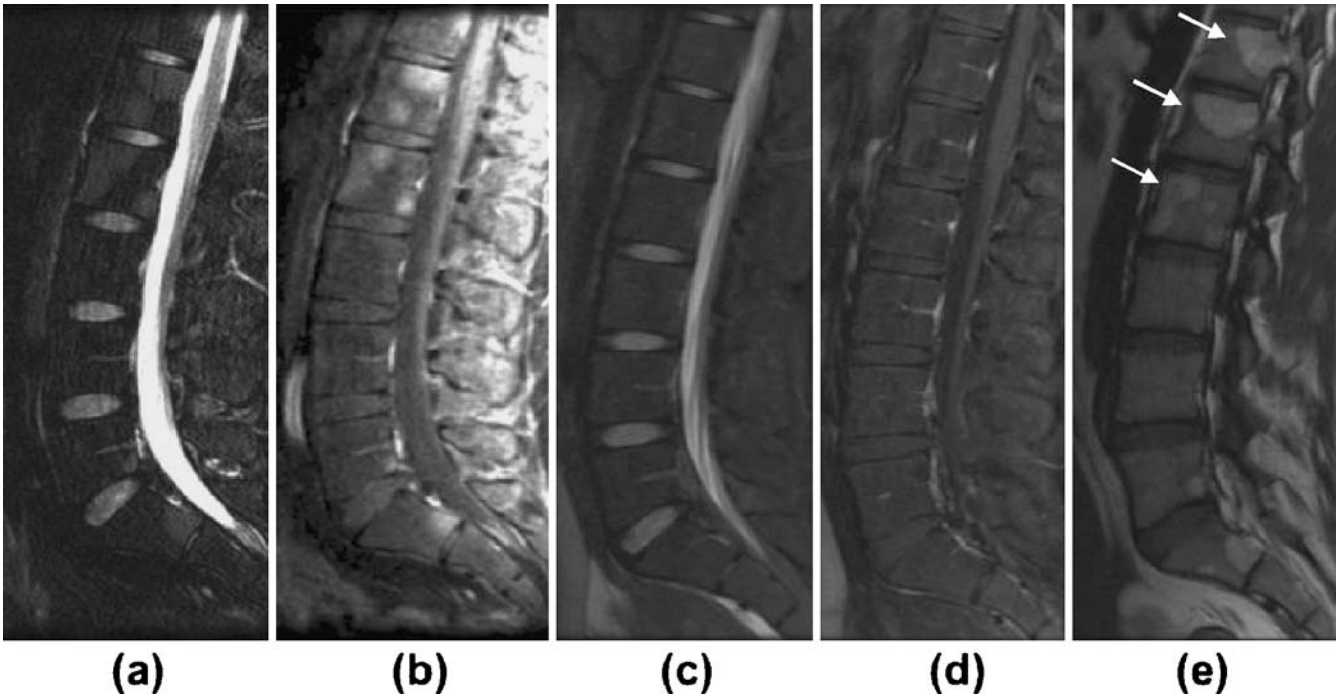

Fig. 7 Sagittal MR images of a patient with malignant lymphoma and multifocal bone marrow infiltration. Sagittal STIR (**a**) and contrast enhanced fat saturated T1-weighted fast SE sequences (700/15–25 ms) were obtained before chemotherapy (**a**, **b**). Fat saturated T2-weighted fast SE (4000/60 ms) ©, contrast enhanced fat saturated T1-weighted fast SE sequences and non-contrast enhanced T1-weighted SE sequences (600/20 ms) were obtained after chemotherapy (**c**–**e**). After therapy, the areas of previous tumor infiltration show a decreased signal on T2-weighted images, a decreased contrast enhancement and fatty degeneration (arrows)

obvious and readily apparent clinical parameters for treatment response.

Treatment effects of various chemotherapeutic regimen on the bone marrow in patients with leukemia and lymphomas could be also detected with 31P MR spectroscopy. A treatment induced change in tumor pH with an alkaline shift was related temporally to increases in the phosphodiester/beta-adenosine triphosphate ratio, and occurred before alterations in tumor size were documented [64]. And interestingly, changes in the 31P MR spectral profile could not only be detected by direct investigations of the bone marrow itself, but also by MR spectroscopy of the serum of the patients. The 31P MR spectral profile of the serum changed in responding patients to resemble that of normal serum with typical, higher peak intensities as compared to non-treated and non-responding patients [65].

Bone marrow reconversion after standard therapy

After successful cytotoxic therapy and/or irradiation, the normal bone marrow may undergo a reconversion from fatty to highly cellular hematopoietic marrow. This reconversion occurs in a reverse fashion compared to the conversion from hematopoietic marrow to fatty marrow, described above, i.e., the reconversion progresses from the central skeleton to the periphery. Within long bones, it involves first the metaphyses and then the diaphyses. The presence of cellular marrow within the epiphyses in an adult patient with hematologic malignancies is always suspicious for neoplastic infiltration, especially when the rest of the bone marrow did not undergo a complete reconversion. A reconversion of marrow within the epiphyses is only rarely seen, usually in conjunction with an extensive reconversion of the hematoietic marrow of the whole bone.

In patients with lymphoma, the reconversion process may be enhanced by administration of granulocyte colony stimulating factor (GCSF), which activates the hematopoietic marrow and decreases the period of aplasia after chemotherapy [66]. The differentiation between this reconverted, highly cellular normal hematopoietic marrow and recurrent tumor after chemotherapy is not possible with conventional MR techniques, since relaxation rates and MR signal characteristics of highly cellular hematopoietic and highly cellular neoplastic bone marrow are similar [67]. Various investigators have addressed this problem, but were not able to differentiate reconverted hypercellular hematopoietic marrow and tumor infiltration using a variety of pulse sequences, static post-contrast MR images, and MR spectroscopy (Fig. 8) [66, 68].

Dynamic T1-weighted MR images after intravenous bolus injection of standard small molecular Gd-chelates may be helpful in the differentiation between normal

Fig. 8 A patient with myeloma at different stages of therapy. **a**) After chemotherapy and irradiation, the bone marrow of the pelvis and proximal femurs shows a major fatty conversion with small areas of hypointense, cellular marrow of uncertain significance on plain T1-weighted MR images. **b**) After high-dose chemotherapy and GCSF treatment, several areas of hypercellular, hypointense marrow are seen in the marrow of the pelvis and proximal femurs. The lower row of images shows that these areas appear bright on FS-T2-w images (b1), hypointense on plain T1-w images (b2) and show a marked enhancement on Gd-enhanced T1-w scans (b3). A follow up study, 3 months after the study in (**c**), shows again a fatty conversion of the bone marrow. In retrospect, the lesions in B were most likely due to reconverted hematopoietic marrow

hypercellular hematopoietic and neoplastic marrow. When compared with red marrow, enhancement of abnormal bone marrow occurred earlier, was steeper and did not last as long in neoplastic bone marrow infiltrations [69–71]. However, in our experience, the Gd-enhancement of the GCSF-treated, markedly hypercellular marrow and neoplastic marrow in patients with hematologic malignancies shows considerable overlap and is of limited clinical value for a definitive differentiation of these entities.

USPIO contrast agents may be more useful for such a differentiation of reconverted marrow and tumor recurrence. The pathophysiologic basis for this is the distribution of RES cells in the bone marrow and their ability to phagocytose exogenous iron oxides. After chemotherapy, especially after GCSF treatment, the bone marrow reconversion causes an increased quantity of all hematopoietic cell lines in the bone marrow, including RES cells [72]. In bone marrow neoplasia, on the other hand, the hematopoietic marrow is replaced by tumor cells and the number of RES cells is substantially reduced [73]. Thus, USPIO-enhanced MRI can differentiate these entities by depicting iron oxide-targeted RES cells, which are present in the reconverted hematopoietic marrow, but not present or substantially reduced in focal or multifocal tumor deposits [17, 29, 31]. Before USPIO administration, both, the hypercellular hematopoietic and neoplastic marrow appear of low signal intensity on plain T1-weighted MR images and of high signal intensity on STIR and fat saturated T2-weighted MR images (Fig. 8). After USPIO administration, however, the normal marrow, which takes up the USPIO, shows an iron oxide induced signal loss, whereas focal neoplastic marrow infiltrates, which do not take up the USPIO, stand out as bright lesions on STIR and fat saturated T2-weighted MR images (Fig. 9) [17, 29, 31]. The technique can also be applied in case of a diffuse, marked hypercellularity of the bone marrow (Fig. 10). Diffuse or focal cell components of the normal, non-neoplastic bone marrow, which appear iso- or hypointense to intervertebral disks or skeletal muscle on plain T1-weighted MR images do show a substantial signal loss on USPIO-enhanced STIR images. If this signal loss is not observed, a malignant infiltration is present (Fig. 10). On the other hand, a USPIO-administration is not meaningful in patients with a fatty marrow on T1-weighted MR images, because there are obviously no cells present, which could take up these particulate contrast agents. Thus, USPIO may be applied in specific patients, where a differentiation of hypercellular normal marrow and neoplastic infiltration is warranted.

New therapy regimens

Angiogenesis-inhibiting drugs, such as thalidomide, may be useful for treating hematologic malignancies that depend on neovascularization, and these agents were recently added to some treatment regimens for patients with advanced myeloma [74]. The anti-angiogenic therapy is intended to stop cancer progression by suppressing the tumor recruitment of new blood supply. As such, the anti-

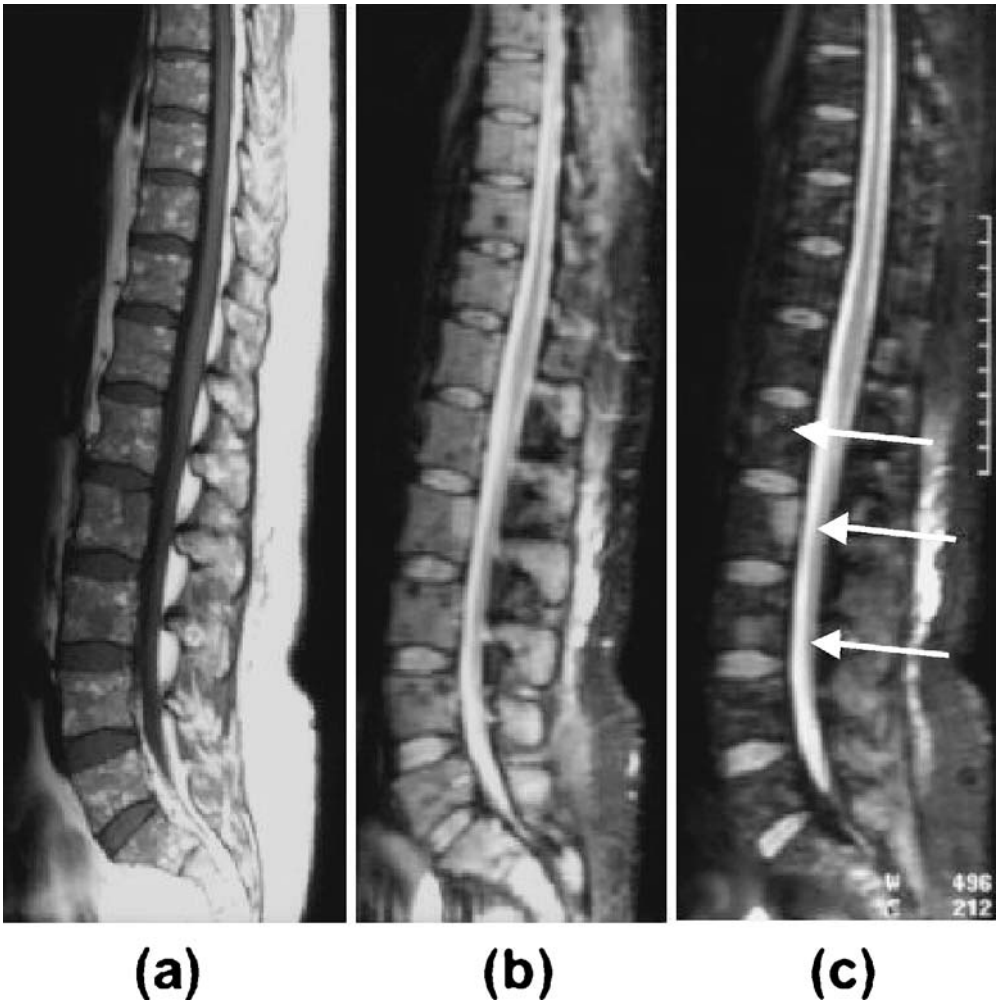

Fig. 9 A 42-year-old patient after recurrent chemotherapy and GCSF treatment with re-converted, hyperplastic hematopoietic marrow and multifocal bone marrow infiltration by lymphoma. Both hematopoietic marrow and focal tumor infiltration show a low signal intensity on plain T1-weighted images (**a**), as well as an increased signal intensity on plain STIR images (**b**); however, STIR images after iron oxide administration (**c**) show a marked signal decrease of the hematopoietic marrow, whereas focal tumors (arrows) do not show any iron oxide uptake; thus, the tumor-to-bone marrow contrast increases substantially (figure from [31])

angiogenic drugs are generally tumorostatic, not cytotoxic. Thus, a successful therapeutic inhibition of angiogenesis can be expected to slow or stop tumor growth, but not to cause tumor regression or disappearance. Accordingly, MR imaging may show a persistent high bone marrow cellularity under anti-angiogenic treatment. Signs of a response to this treatment are rather a delayed, less steep and smaller bone marrow enhancement after intravenous administration of small molecular Gd-chelates compared to pretreatment studies.

New macromolecular contrast agents (MMCM) may provide an earlier diagnosis of response or failure of anti-angiogenic treatment than standard small molecular contrast agents. MMCM are more sensitive in the detection of changes in vascular permeability than small molecular contrast agents. And such changes in the permeability of bone marrow sinus occurs earlier than changes in perfusion and blood volume, typically assessed with small molecular contrast agents. In animal models, MMCM-enhanced MRI was able to define anti-VEGF effects of certain angiogenesis inhibitors as early as one day after initiation of therapy [75, 76]. Future studies have to show, if these results can be also obtained in patients and if so, they would be obviously of high clinical significance for treatment monitoring and management.

In clinical practice, anti-angiogenic therapy regimens will almost certainly combine anti-angiogenic drugs with cytotoxic drugs. The effect of such combined therapies on the tumor accumulation and therapeutic effect of the individual drugs are complex and currently investigated in several experimental and clinical trials. Again, imaging techniques are the only available tool to provide a non-invasive and serial assessment of such combined therapy regimens. Some angiogenesis inhibitors, such as anti-VEGF antibody, decrease microvessel permeability and thereby reduce tumoral delivery of large molecular cytotoxic drugs, but not small molecular cytotoxic drugs [76]. MRI assays of angiogenesis can monitor such anti-angiogenesis therapy induced changes in tumor microvascular structure and optimize the choice and timing of cytotoxic drug administration. Other inhibitors of angiogenesis, such as anti-angiogenic steroids (tetrahydrocortisol, cortisone acetate), cyclodextrin derivates 460 (cyclodextrin tetradecasulfate), and tetracycline derivates

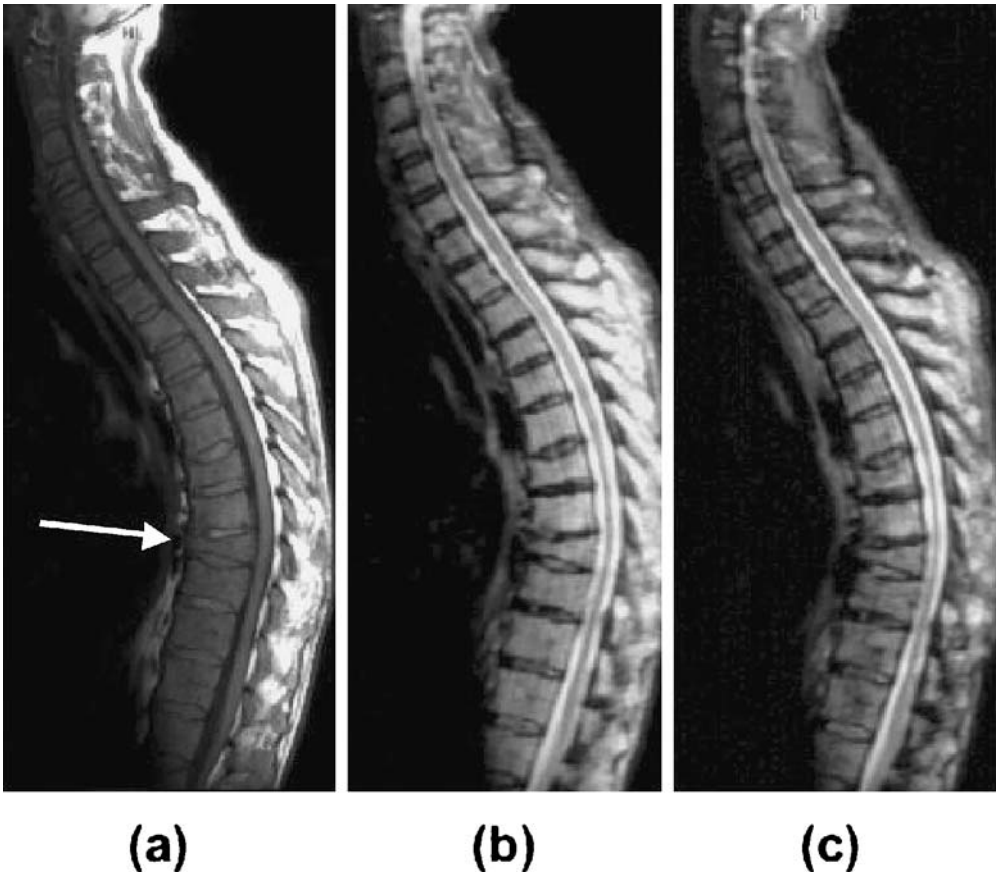

Fig. 10 A 57-year-old patient with myeloma after chemotherapy and GCSF treatment. T1-weighted images before (**a**) show a pathologic fracture of Th 9 (arrow) and a diffuse hypointense signal intensity of the bone marrow in all vertebrae, compatible with a high bone marrow cellularity. Unenhanced STIR images (**b**) show a diffuse hyperintense bone marrow, also compatible with high bone marrow cellularity. After iron oxide infusion, the hypercellular bone marrow shows only minimal changes in signal intensity on STIR images (**c**), indicative of a diffuse tumor infiltration. Iliac crest biopsy revealed 80% tumor cells in the bone marrow (figure from [31])

(minocycline), may increase tumor microvascular permeability and thus potentiate certain cytotoxic therapies [77, 78]. In addition, inhibitors of angiogenesis have been shown to effectively potentiate tumor irradiation effects [79]. This possible synergy between these anti-angiogenesis drugs and cytotoxic drugs or irradiation, as a function of apparent tumor microvascular hyperpermeability, can also be interrogated with MMCM-enhanced MR imaging.

Stem cell transplantation

The most commonly used therapy for patients with lymphoma is autologous stem cell transplantation. For this, the patient receives a conditioning therapy, then his or her own stem cells are collected by leukapheresis, the patient subsequently receives a high-dose chemotherapy or irradiation and his previously collected stem cells are reinfused. With some types of lymphoma, an autologous transplant may not be possible in case of persistent malignant bone marrow infiltration. Even after purging (treatment of the stem cells in the lab to kill or remove lymphoma cells), reinfusion of some lymphoma cells with the stem cell transplant is possible. It would, therefore, be of high clinical significance to be able to differentiate patients with still viable lymphoma cells in their bone marrow at the time of leukapheresis from patients in true complete remission.

In refractory diseases or in aplastic anemia, allogenic marrow transplantation or chord cell transplantation are also used. This much more aggressive procedure is initiated by a conditioning high dose chemotherapy and/or total body irradiation and subsequent reinfusion of allogenic donor cells, i.e., stem cells from a matched sibling or unrelated donor. Allogenic transplantation has limited applications, because of the need for a matched donor. Another drawback is that side effects of this treatment are too severe for most people over 55 years old. After the conditioning therapy for allogenic marrow transplantation, the patients reach complete aplasia, are usually isolated on a bone marrow transplantation unit and should only undergo MR imaging for vital indications.

Only limited studies exist about the evaluation of bone marrow with MR imaging in the setting of bone marrow transplantation in patients with hematologic disorders. Based on these data, the MR imaging characteristics of the bone marrow after autologous or allogenic marrow transplantation are apparently quite similar [80].

After the conditioning therapy and before bone marrow transplantation, the bone marrow would be assumed to be depleted of tumor cells. Ideally, a conversion from focal or diffuse hypercellular marrow to normocellular or fatty

marrow would be expected to occur after the induction high-dose chemotherapy. However, MR studies in patients before bone marrow transplantation showed that some patients have persistent focal lesions. Metz et al. described residual focal bone marrow lesions in patients with lymphomas right before leukapheresis [17]. Negendak and Soulen found that patients with residual lesions on MR before bone marrow transplantation had a significantly shorter median time until relapse compared to patients who did not show any residual bone marrow disease on MR images [81]. By contrast, Lecouvet et al. reported that patients with an apparently normal marrow and patients with a persistent pathologic bone marrow right before autologous or allogenic transplantation did not show differences in survival [80]. One reason for this difference in observation may be the limitation of the MR imaging technique to detect and differentiate viable and non-viable tumor cells. Some patients with a "clean" bone marrow may have residual microscopic active tumor cells while macroscopic residual lesions on MR imaging in other patients may or may not be viable. In our opinion, it would be highly significant to investigate MR imaging criteria (e.g., diffusion weighted MR, dynamic MR, new contrast agents, spectroscopy) for the differentiation of such persistent focal bone marrow lesions that may or may not develop to recurrent disease after stem cell transplantation.

After bone marrow transplantation, the evolution of distinct MR signal patterns of the bone marrow has been described [82, 83]. During the first post-transplantation days, the bone marrow shows a decline in signal intensity on T1-weighted images and an increased signal intensity on T2-weighted images, probably due to a treatment-induced edema. Within 3 months from bone marrow transplantation, a characteristic band pattern appears on T1-weighted MR images of the spine. This band pattern consists of a peripheral T1-hypointense zone and a central T1-hyperintense zone. At histologic examination, the peripheral zone corresponded to repopulating hematopoietic marrow and the central zone to marrow fat. This "band pattern" may be seen for several months [82, 83]. Subsequently, the band pattern gradually evolves into a homogeneous appearance of the marrow after successful bone marrow transplantation. On late post-transplant MR studies, years after bone marrow transplantation, the bone marrow shows the fatty conversion of adult marrow. The signal intensity of the post-transplant bone marrow on T1-weighted MR images is usually increased compared to age-matched controls [84].

In some patients, residual marrow abnormalities may be observed on MR images after bone marrow transplantation and the administration of high-dose myeloablative chemotherapy, in the same way that they may occur after conventional chemotherapy and conditioning chemotherapy regimens, described above (Fig. 11). For example, sharply defined focal low signal intensity areas of bone marrow on T1-weighted images have been reported in patients who are in complete remission after transplantation [85]. Patients with these abnormalities did not have a poorer outcome than those with normal post-transplantation MR imaging findings [80]. These data show that there is clearly a need for the MR imaging technique to add some functional information to the anatomical data, e.g., by adding spectroscopy, perfusion studies or markers for tumor cell proliferation.

Of note, iron overload commonly accompanies bone marrow transplantation and may result in a diffusely decreased signal intensity of the liver (reported in 77% of pediatric cases after bone marrow transplantation), spleen (46%) and bone marrow (38.5%) on T2-weighted and

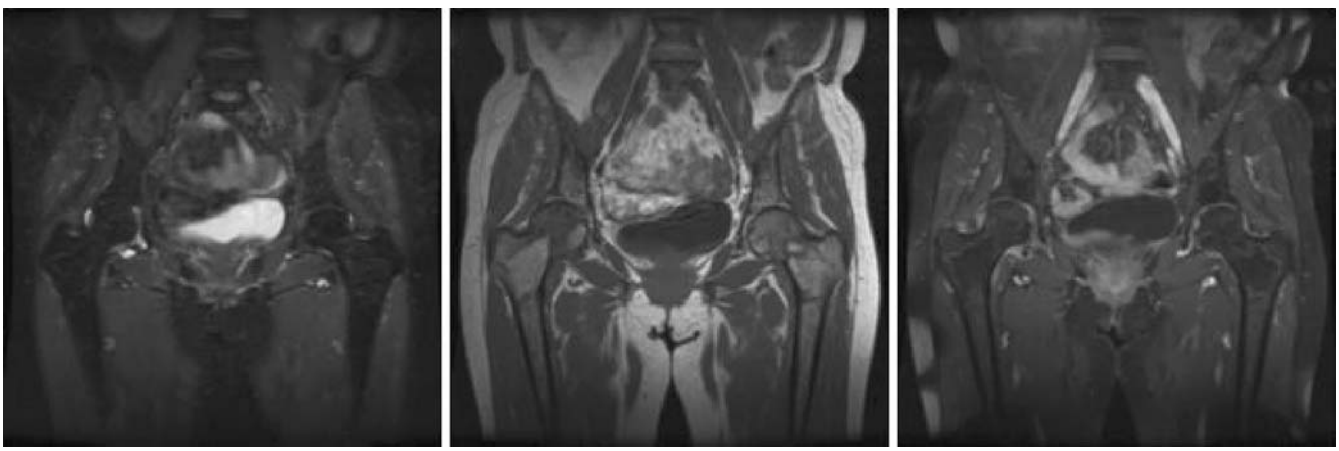

Fig. 11 Patient with malignant lymphoma after TBI and bone marrow transplantation: Plain T1-w MR image (center) shows residual hypointense bone marrow lesions in the pelvis and proximal femur. Some of these lesions may be residual marrow abnormalities of uncertain significance. Other lesions, such as the serpiginous lesions in both proximal femurs represent therapy-induced bone infarcts. These lesions show a corresponding serpiginous hyperintense area on STIR images (left) and a minor, serpiginous enhancement on Gd-enhanced T1-w scans (right)

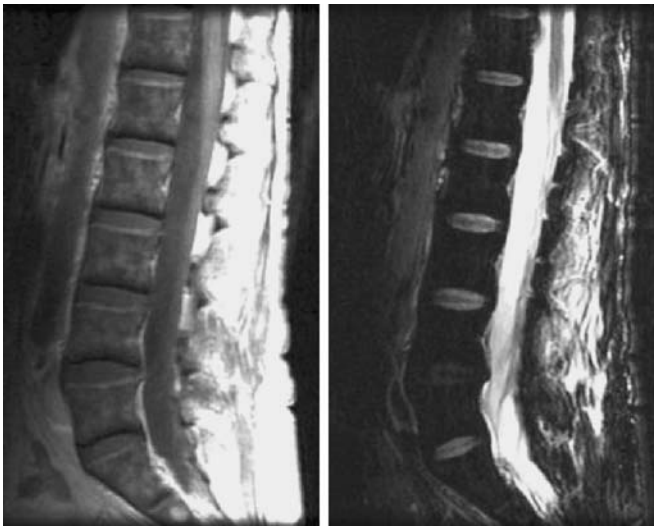

Fig. 12 A patient with myeloma after bone marrow transplantation: The bone marrow of the lumbar spine shows a diffuse hypointense signal intensity on both plain T1-weighted (left) and fat-saturated T2-weighted (right) MR images

STIR MR images (Fig. 12). The degree of hepatic iron overload correlated significantly and splenic iron overload correlated weakly with the number of blood transfusions [86].

TBI can cause irradiation induced signal changes and complications, described above (Fig. 11). Long-term complications of TBI, applied as part of the conditioning regimen for a bone marrow transplantation, are the development of osteochondromas or sarcomas.

In summary, MR imaging can be a useful tool to aid in the treatment monitoring of patients with hematologic malignancies by monitoring treatment response, detecting treatment complications, differentiating normal and neoplastic hypercellular marrow and by diagnosing residual or recurrent tumor deposits. In order to achieve clinical significance and cost-effectiveness, the MR imaging technique should be clearly tailored to specific patients and the specific questions described in detail above. New MR imaging techniques may serve to depict those molecular pathways and regulatory events that control blood vessel growth and proliferation. Non-invasive monitoring of anti-angiogenic therapies has found success by defining tumor microvascular and metabolic changes, while treatment-related changes in bone marrow morphology tend to occur rather late and are non-specific. Already established in many institutions, future developments will almost certainly include "fusion" or "hybrid" imaging methods, such as PET-CT and PET-MR in the treatment monitoring of patients with malignant lymphomas.

References

1. Plecha DM (2000) Imaging of bone marrow disease in the spine. Semin Musculoskelet Radiol 4:321–327
2. Durie BG, Salmon SE (1975) A clinical staging system for multiple myeloma. Correlation of measured myeloma cell mass with presenting clinical features, response to treatment, and survival. Cancer 36:842–854
3. Coller BS, Chabner BA, Gralnick HR (1977) Frequencies and patterns of bone marrow involvement in non-Hodgkin lymphomas: observations on the value of bilateral biopsies. Am J Hematol 3:105–119
4. Brunning RD, Bloomfield CD, McKenna RW, Peterson LA (1975) Bilateral trephine bone marrow biopsies in lymphoma and other neoplastic diseases. Ann Intern Med 82:365–366
5. Schirrmeister H, Bommer M, Buck AK, Muller S, Messer P, Bunjes D, Dohner H, Bergmann L, Reske SN (2002) Initial results in the assessment of multiple myeloma using 18F-FDG PET. Eur J Nucl Med Mol Imaging 29:361–366
6. Lecouvet FE, Malghem J, Michaux L, Maldague B, Ferrant A, Michaux JL, Vande Berg BC (1999) Skeletal survey in advanced multiple myeloma: radiographic versus MR imaging survey. Br J Haematol 106:35–39
7. Baur A, Stabler A, Nagel D, Lamerz R, Bartl R, Hiller E, Wendtner C, Bachner F, Reiser M (2002) Magnetic resonance imaging as a supplement for the clinical staging system of Durie and Salmon? Cancer 95:1334–1345
8. Dimopoulos MA, Moulopoulos A, Smith T, Delasalle KB, Alexanian R (1993) Risk of disease progression in asymptomatic multiple myeloma. Am J Med 94:57–61
9. Van de Berg BC, Lecouvet FE, Michaux L, Labaisse M, Malghem J, Jamart J, Maldague BE, Ferrant A, Michaux JL (1996) Stage I multiple myeloma: value of MR imaging of the bone marrow in the determination of prognosis. Radiology 201:243–246
10. Smith DB, Scarffe JH, Eddleston B (1988) The prognostic significance of X-ray changes at presentation and reassessment in patients with multiple myeloma. Hematol Oncol 6:1–6
11. Moulopoulos LA, Varma DG, Dimopoulos MA, Leeds NE, Kim EE, Johnston DA, Alexanian R, Libshitz HI (1992) Multiple myeloma: spinal MR imaging in patients with untreated newly diagnosed disease. Radiology 185:833–840
12. Hoane BR, Shields AF, Porter BA, Shulman HM (1991) Detection of lymphomatous bone marrow involvement with magnetic resonance imaging. Blood 78:728–738
13. Tsunoda S, Takagi S, Tanaka O, Miura Y (1997) Clinical and prognostic significance of femoral marrow magnetic resonance imaging in patients with malignant lymphoma. Blood 89:286–290
14. Munk PL, Helms CA, Holt RG (1989) Immature bone infarcts: findings on plain radiographs and MR scans. Am J Roentgenol 152:547–549
15. Ishibashi Y, Okamura Y, Otsuka H, Nishizawa K, Sasaki T, Toh S (2002) Comparison of scintigraphy and magnetic resonance imaging for stress injuries of bone. Clin J Sport Med 12:79–84

16. Ghanem N, Lohrmann C, Engelhardt M, Pache G, Uhl M, Saueressig U, Kotter E, Langer M (2006) Whole-body MRI in the detection of bone marrow infiltration in patients with plasma cell neoplasms in comparison to the radiological skeletal survey. Eur Radiol 16:1005–1014
17. Metz S, Lohr S, Settles M, Beer A, Woertler K, Rummeny EJ, Daldrup-Link HE (2006) Ferumoxtran-10-enhanced MR imaging of the bone marrow before and after conditioning therapy in patients with non-Hodgkin lymphomas. Eur Radiol 16:598–607
18. Delfaut EM, Beltran J, Johnson G, Rousseau J, Marchandise X, Cotten A (1999) Fat suppression in MR imaging: techniques and pitfalls. Radiographics 19:373–382
19. Rahmouni A, Montazel JL, Divine M, Lepage E, Belhadj K, Gaulard P, Bouanane M, Golli M, Kobeiter H (2003) Bone marrow with diffuse tumor infiltration in patients with lymphoproliferative diseases: dynamic gadolinium-enhanced MR imaging. Radiology 229:710–717
20. Baur A, Stabler A, Bruning R, Bartl R, Krodel A, Reiser M, Deimling M (1998) Diffusion-weighted MR imaging of bone marrow: differentiation of benign versus pathologic compression fractures. Radiology 207:349–356
21. Ballon D, Watts R, Dyke JP, Lis E, Morris MJ, Scher HI, Ulug AM, Jakubowski AA (2004) Imaging therapeutic response in human bone marrow using rapid whole-body MRI. Magn Reson Med 52:1234–1238
22. Vacca A, Ribatti D, Roncali L, Ranieri G, Serio G, Silvestris F, Dammacco F (1994) Bone marrow angiogenesis and progression in multiple myeloma. Br J Haematol 87:503–508
23. Rahmouni A, Tempany C, Jones R, Mann R, Yang A, Zerhouni E (1993) Lymphoma: monitoring tumor size and signal intensity with MR imaging. Radiology 188:445–451
24. Vande Berg BC, Lecouvet FE, Galant C, Maldague BE, Malghem J (2005) Normal variants and frequent marrow alterations that simulate bone marrow lesions at MR imaging. Radiol Clin North Am 43:761–770, ix
25. Montazel JL, Divine M, Lepage E, Kobeiter H, Breil S, Rahmouni A (2003) Normal spinal bone marrow in adults: dynamic gadolinium-enhanced MR imaging. Radiology 229:703–709
26. Baur A, Stabler A, Bartl R, Lamerz R, Scheidler J, Reiser M (1997) MRI gadolinium enhancement of bone marrow: age-related changes in normals and in diffuse neoplastic infiltration. Skeletal Radiol 26:414–418
27. Daldrup-Link HE, Link TM, Rummeny EJ, August C, Konemann S, Jurgens H, Heindel W (2000) Assessing permeability alterations of the blood-bone marrow barrier due to total body irradiation: in vivo quantification with contrast enhanced magnetic resonance imaging. Bone Marrow Transplant 25:71–78
28. Seneterre E, Weissleder R, Jaramillo D, Reimer P, Lee AS, Brady TJ, Wittenberg J (1991) Bone marrow: ultrasmall superparamagnetic iron oxide for MR imaging. Radiology 179:529–533
29. Bush CH, Mladinich CR, Montgomery WJ (1997) Evaluation of an ultrasmall superparamagnetic iron oxide in MRI in a bone tumor model in rabbits. J Magn Reson Imaging 7:579–584
30. Simon GH, Raatschen HJ, Wendland MF, von Vopelius-Feldt J, Fu Y, Chen MH, Daldrup-Link HE (2005) Ultrasmall superparamagnetic iron-oxide-enhanced MR imaging of normal bone marrow in rodents: original research original research. Acad Radiol 12:1190–1197
31. Daldrup-Link HE, Rummeny EJ, Ihssen B, Kienast J, Link TM (2002) Iron-oxide-enhanced MR imaging of bone marrow in patients with non-Hodgkin's lymphoma: differentiation between tumor infiltration and hypercellular bone marrow. Eur Radiol 12:1557–1566
32. Wang CK, Li CW, Hsieh TJ, Chien SH, Liu GC, Tsai KB (2004) Characterization of bone and soft-tissue tumors with in vivo 1H MR spectroscopy: initial results. Radiology 232:599–605
33. Somer EJ, Marsden PK, Benatar NA, Goodey J, O'Doherty MJ, Smith MA (2003) PET-MR image fusion in soft tissue sarcoma: accuracy, reliability and practicality of interactive point-based and automated mutual information techniques. Eur J Nucl Med Mol Imaging 30:54–62
34. Pichler BJ, Judenhofer MS, Catana C, Walton JH, Kneilling M, Nutt RE, Siegel SB, Claussen CD, Cherry SR (2006) Performance Test of an LSO-APD Detector in a 7-T MRI Scanner for Simultaneous PET/MRI. J Nucl Med 47:639–647
35. Babyn PS, Ranson M, McCarville ME (1998) Normal bone marrow: signal characteristics and fatty conversion. Magn Reson Imaging Clin N Am 6:473–495
36. Zawin JK, Jaramillo D (1993) Conversion of bone marrow in the humerus, sternum, and clavicle: changes with age on MR images. Radiology 188:159–164
37. Ricci C, Cova M, Kang YS, Yang A, Rahmouni A, Scott WW Jr, Zerhouni EA (1990) Normal age-related patterns of cellular and fatty bone marrow distribution in the axial skeleton: MR imaging study. Radiology 177:83–88
38. Moore SG, Dawson KL (1990) Red and yellow marrow in the femur: age-related changes in appearance at MR imaging. Radiology 175:219–223
39. Wasser K, Moehler T, Nosas-Garcia S, Rehm C, Bartl R, Goldschmidt H, Duber C, Kauczor HU, Delorme S (2005) Correlation of MRI and histopathology of bone marrow in patients with multiple myeloma. Rofo 177:1116–1122
40. Lecouvet FE, Vande Berg BC, Michaux L, Malghem J, Maldague BE, Jamart J, Ferrant A, Michaux JL (1998) Stage III multiple myeloma: clinical and prognostic value of spinal bone marrow MR imaging. Radiology 209:653–660
41. Moehler TM, Hawighorst H, Neben K, Egerer G, Hillengass J, Max R, Benner A, Ho AD, van Kaick G, Goldschmidt H (2001) Bone marrow microcirculation analysis in multiple myeloma by contrast-enhanced dynamic magnetic resonance imaging. Int J Cancer 93:862–868
42. Nosas-Garcia S, Moehler T, Wasser K, Kiessling F, Bartl R, Zuna I, Hillengass J, Goldschmidt H, Kauczor HU, Delorme S (2005) Dynamic contrast-enhanced MRI for assessing the disease activity of multiple myeloma: a comparative study with histology and clinical markers. J Magn Reson Imaging 22:154–162
43. Stabler A, Baur A, Bartl R, Munker R, Lamerz R, Reiser MF (1996) Contrast enhancement and quantitative signal analysis in MR imaging of multiple myeloma: assessment of focal and diffuse growth patterns in marrow correlated with biopsies and survival rates. Am J Roentgenol 167:1029–1036
44. Yankelevitz DF, Henschke CI, Knapp PH, Nisce L, Yi Y, Cahill P (1991) Effect of radiation therapy on thoracic and lumbar bone marrow: evaluation with MR imaging. Am J Roentgenol 157:87–92
45. Otake S, Mayr NA, Ueda T, Magnotta VA, Yuh WT (2002) Radiation-induced changes in MR signal intensity and contrast enhancement of lumbosacral vertebrae: do changes occur only inside the radiation therapy field? Radiology 222:179–183

46. Blomlie V, Rofstad EK, Skjonsberg A, Tvera K, Lien HH (1995) Female pelvic bone marrow: serial MR imaging before, during, and after radiation therapy. Radiology 194:537–543
47. Roebuck DJ (1999) Skeletal complications in pediatric oncology patients. Radiographics 19:873–885
48. Fletcher BD, Crom DB, Krance RA, Kun LE (1994) Radiation-induced bone abnormalities after bone marrow transplantation for childhood leukemia. Radiology 191:231–235
49. Perez CA, Vietti T, Ackerman LV, Eagleton MD, Powers WE (1967) Tumors of the sympathetic nervous system in children. An appraisal of treatment and results. Radiology 88:750–760
50. Maghami EG, St-John M, Bhuta S, Abemayor E (2005) Postirradiation sarcoma: a case report and current review. Am J Otolaryngol 26:71–74
51. Tountas AA, Fornasier VL, Harwood AR, Leung PM (1979) Postirradiation sarcoma of bone: a perspective. Cancer 43:182–187
52. Iida S, Harada Y, Shimizu K, Sakamoto M, Ikenoue S, Akita T, Kitahara H, Moriya H (2000) Correlation between bone marrow edema and collapse of the femoral head in steroid-induced osteonecrosis. Am J Roentgenol 174:735–743
53. Turner DA, Templeton AC, Selzer PM, Rosenberg AG, Petasnick JP (1989) Femoral capital osteonecrosis: MR finding of diffuse marrow abnormalities without focal lesions. Radiology 171:135–140
54. Mitchell DG, Rao VM, Dalinka MK, Spritzer CE, Alavi A, Steinberg ME, Fallon M, Kressel HY (1987) Femoral head avascular necrosis: correlation of MR imaging, radiographic staging, radionuclide imaging, and clinical findings. Radiology 162:709–715
55. Maheshwari PR, Nagar AM, Prasad SS, Shah JR, Patkar DP (2004) Avascular necrosis of spine: a rare appearance. Spine 29:E119–E122
56. Gerard EL, Ferry JA, Amrein PC, Harmon DC, McKinstry RC, Hoppel BE, Rosen BR (1992) Compositional changes in vertebral bone marrow during treatment for acute leukemia: assessment with quantitative chemical shift imaging. Radiology 183:39–46
57. Islam A, Catovsky D, Galton DA (1980) Histological study of bone marrow regeneration following chemotherapy for acute myeloid leukaemia and chronic granulocytic leukaemia in blast transformation. Br J Haematol 45:535–540
58. Moulopoulos LA, Dimopoulos MA, Alexanian R, Leeds NE, Libshitz HI (1994) Multiple myeloma: MR patterns of response to treatment. Radiology 193:441–446
59. Zinzani PL (2005) Lymphoma: diagnosis, staging, natural history, and treatment strategies. Semin Oncol 32: S4–S10
60. Rahmouni A, Divine M, Mathieu D, Golli M, Haioun C, Dao T, Anglade MC, Reyes F, Vasile N (1993) MR appearance of multiple myeloma of the spine before and after treatment. Am J Roentgenol 160:1053–1057
61. Lien HH, Holte H (1996) Fat replacement of Hodgkin disease of bone marrow after chemotherapy: report of three cases. Skeletal Radiol 25:671–674
62. Fassas AB, Muwalla F, Berryman T, Benramdane R, Joseph L, Anaissie E, Sethi R, Desikan R, Siegel D, Badros A, Toor A, Zangari M, Morris C, Angtuaco E, Mathew S, Wilson C, Hough A, Harik S, Barlogie B, Tricot G (2002) Myeloma of the central nervous system: association with high-risk chromosomal abnormalities, plasmablastic morphology and extramedullary manifestations. Br J Haematol 117:103–108
63. Angtuaco EJ, Fassas AB, Walker R, Sethi R, Barlogie B (2004) Multiple myeloma: clinical review and diagnostic imaging. Radiology 231:11–23
64. Smith SR, Martin PA, Edwards RH (1991) tumor pH and response to chemotherapy: an in vivo 31P magnetic resonance spectroscopy study in non-Hodgkin's lymphoma. Br J Radiol 64:923–928
65. Kuliszkiewicz-Janus M, Baczynski S, Jurczyk A (2004) Bone marrow transplantation in the course of hematological malignancies-follow-up study in blood serum by 31P MRS. Med Sci Monit 10:CR485–CR492
66. Fletcher BD, Wall JE, Hanna SL (1993) Effect of hematopoietic growth factors on MR images of bone marrow in children undergoing chemotherapy. Radiology 189:745–751
67. Layer G, Sander W, Traber F, Block W, Ko Y, Ziske CG, Konig R, Vahlensieck M, Schild HH (2000) The diagnostic problems in magnetic resonance tomography of the bone marrow in patients with malignomas under G-CSF therapy. Radiologe 40:710–715
68. Vanel D, Missenard G, Le Cesne A, Guinebretiere JM (1997) Red marrow recolonization induced by growth factors mimicking an increase in tumor volume during preoperative chemotherapy: MR study. J Comput Assist Tomogr 21:529–531
69. Hawighorst H, Libicher M, Knopp MV, Moehler T, Kauffmann GW, Kaick G (1999) Evaluation of angiogenesis and perfusion of bone marrow lesions: role of semiquantitative and quantitative dynamic MRI. J Magn Reson Imaging 10:286–294
70. Bollow M, Knauf W, Korfel A, Taupitz M, Schilling A, Wolf KJ, Hamm B (1997) Initial experience with dynamic MR imaging in evaluation of normal bone marrow versus malignant bone marrow infiltrations in humans. J Magn Reson Imaging 7:241–250
71. Moulopoulos LA, Maris TG, Papanikolaou N, Panagi G, Vlahos L, Dimopoulos MA (2003) Detection of malignant bone marrow involvement with dynamic contrast-enhanced magnetic resonance imaging. Ann Oncol 14:152–158
72. Lieschke GJ, Burgess AW (1992) Granulocyte colony-stimulating factor and granulocyte-macrophage colony-stimulating factor (1). N Engl J Med 327:28–35
73. Vande Berg BC, Lecouvet FE, Kanku JP, Jamart J, Van Beers BE, Maldague B, Malghem J (1999) Ferumoxides-enhanced quantitative magnetic resonance imaging of the normal and abnormal bone marrow: preliminary assessment. J Magn Reson Imaging 9:322–328
74. Singhal S, Mehta J, Desikan R, Ayers D, Roberson P, Eddlemon P, Munshi N, Anaissie E, Wilson C, Dhodapkar M, Zeddis J, Barlogie B (1999) Antitumor activity of thalidomide in refractory multiple myeloma. N Engl J Med 341:1565–1571
75. Pham CD, Roberts TP, van Bruggen N, Melnyk O, Mann J, Ferrara N, Cohen RL, Brasch RC (1998) Magnetic resonance imaging detects suppression of tumor vascular permeability after administration of antibody to vascular endothelial growth factor. Cancer Invest 16:225–230
76. Daldrup-Link HE, Okuhata Y, Wolfe A, Srivastav S, Oie S, Ferrara N, Cohen RL, Shames DM, Brasch RC (2004) Decrease in tumor apparent permeability-surface area product to a MRI macromolecular contrast medium following angiogenesis inhibition with correlations to cytotoxic drug accumulation. Microcirculation 11:387–396
77. Teicher BA, Sotomayor EA, Huang ZD (1992) Antiangiogenic agents potentiate cytotoxic cancer therapies against primary and metastatic disease. Cancer Res 52:6702–6704

78. Lee K, Erturk E, Mayer R, Cockett AT (1987) Efficacy of antitumor chemotherapy in C3H mice enhanced by the antiangiogenesis steroid, cortisone acetate. Cancer Res 47:5021–5024
79. Gali-Muhtasib H, Sidani M, Geara F, Mona AD, Al-Hmaira J, Haddadin MJ, Zaatari G (2004) Quinoxaline 1,4-dioxides are novel angiogenesis inhibitors that potentiate antitumor effects of ionizing radiation. Int J Oncol 24:1121–1131
80. Lecouvet FE, Dechambre S, Malghem J, Ferrant A, Vande Berg BC, Maldague B (2001) Bone marrow transplantation in patients with multiple myeloma: prognostic significance of MR imaging. Am J Roentgenol 176:91–96
81. Negendank W, Soulen RL (1993) Magnetic resonance imaging in patients with bone marrow disorders. Leuk Lymphoma 10:287–298
82. Stevens SK, Moore SG, Amylon MD (1990) Repopulation of marrow after transplantation: MR imaging with pathologic correlation. Radiology 175:213–218
83. Moulopoulos LA, Dimopoulos MA (1997) Magnetic resonance imaging of the bone marrow in hematologic malignancies. Blood 90:2127–2147
84. Tanner SF, Clarke J, Leach MO, Mesbahi MH, Nicolson V, Powles R, Husband JE, Tait D (1996) MRI in the evaluation of late bone marrow changes following bone marrow transplantation. Br J Radiol 69:1145–1151
85. Lien HH, Blomlie V, Blystad AK, Holte H, Langholm R, Kvaloy S (1997) Bone-marrow MR imaging before and after autologous marrow transplantation in lymphoma patients without known bone-marrow involvement. Acta Radiol 38:896–902
86. Kornreich L, Horev G, Yaniv I, Stein J, Grunebaum M, Zaizov R (1997) Iron overload following bone marrow transplantation in children: MR findings. Pediatr Radiol 27:869–872